

**A.L. Virovlyansky, A.Yu. Kazarova, L.Ya. Lyubavin**  
**ON THE USE OF A VERTICAL ANTENNA FOR RESOLVING PULSE**  
**SIGNALS AT LONG RANGES UNDER CONDITIONS OF RAY CHAOS**

Institute of Applied Physics RAS  
Ulyanov St. 46, Nizhny Novgorod, 603950 Russia 603950  
Tel.: (8312) 16-47-84; Fax: (8312) 35-46-57  
E-mail: viro@hydro.appl.sci-nnov.ru

*Most schemes of acoustic monitoring of temperature fields in the ocean are based on measuring variations of the so-called ray travel times, that is arrival times of sound pulses coming through different ray paths connecting the source and receiver. If signals are registered by a point source, only sound pulses arriving through steep rays can be resolved. This fact strongly complicates solving the inverse problem. To a significant extent this difficulty is caused by the phenomenon of ray chaos. The latter is well developed at ranges on the order of thousand kilometers. In the present work it is shown that the use of a vertical receiving array may help to measure time delays of pulses coming through flat rays. We discuss a spatio-temporal processing of received signals based on the presence of features in the distribution of ray arrivals in the time-depth plane that remain stable even under conditions of ray chaos.*

It is known that only sound pulses propagating at multimegameter ranges along steep ray paths may come to an observation point without overlapping [1]. The use of a vertical array with a narrow directional diagram may help in both enhancing the signal-to-noise ratio and resolving pulses coming through rays with close travel times but significantly different arrival angles. However at frequencies on the order of 100 Hz widely used in experiments on long range sound propagation in the ocean the width of a directional diagram typically exceeds an angular interval between arrival angles of neighboring – especially flat – rays. Therefore the beamforming hardly can help in resolving rays with close travel times and close arrival angles. In the present work we consider an alternative spatio-temporal processing that allows one to measure delays of signals coming through not only steep trajectories but through relatively flat ones as well.

Our starting point is the fact that the distribution of arrivals in the time-depth plane, called the timefront, present a rather stable characteristic of the wave field. The timefront is stable with respect to the influence of weak internal-wave-induced sound speed fluctuations giving rise to wave and ray chaos [2]. This statement is illustrated in plots presented in the upper panels of Figs. 1 and 2. These figures show two pieces of a timefront. The latter has been computed for a simple two dimensional environmental model with the sound speed field  $c(r, z) = c_0(z) + \delta c(r, z)$ , where  $r$  is a range,  $z$  is a depth,  $c_0(z)$  is a smooth unperturbed sound speed profile,  $\delta c(r, z)$  is a weak perturbation caused by random internal waves whose statistics is determined by the empirical Garrett-Munk spectrum. The wave field is excited by a point source set near a minimum of  $c_0(z)$ . Solid piece-wise lines depict parts of the timefront in the unperturbed waveguide at a range of 3000 km from the source. Each segment of these lines is formed by rays with equal identifiers  $\pm M$ , where  $\pm$  is the sign of a ray launch angle and  $M$  is the number of ray turning points between the source and observation range [1,2]. Points show parts of the timefront in the perturbed waveguide. Groups of points depicting arrivals of rays with equal identifiers form the so-called *fuzzy* segments. Travel times of rays arriving at the observation point  $(r, z_r)$  are determined by intersections of the timefront with line  $z = z_r$ .

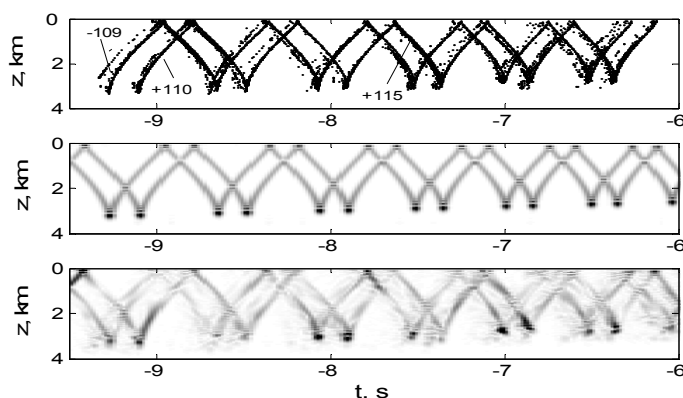


**Fig.1.** *Upper panel:* part of the timefront in the unperturbed (solid lines) and perturbed (points) waveguides; identifiers corresponding to some segments are indicated next to these segments. *Middle panel:* wave field intensity at 3000 km in the time-depth plane in the unperturbed waveguide. *Lower panel:* the same as in the middle panel but for the perturbed waveguide. Travel time is reckoned from the arrival of an axial ray.

The stability of timefront manifests itself in the fact that the segments formed by steep rays in the perturbed and unperturbed waveguide (shown in the upper panel of Fig. 1) are rather close. Similarly, the distribution of signal intensity in the time-depth plane (computed in the parabolic equation approximation) turns out to be stable. The presence of random perturbation comparatively weakly affects this distribution. This is seen from comparison the middle and lower panels in Fig. 1. Results presented in Fig. 2 have been obtained for a piece of the timefront formed by more flat rays. Fuzzy segments become wider but the structure of the perturbed timefront still resembles that in the unperturbed waveguide. At the same time the comparison of the middle and lower panels in Fig. 2 shows that the random perturbation strongly distorts the intensity of the acoustic field. In the lower panel of Fig. 2 it is difficult to distinguish individual segments.

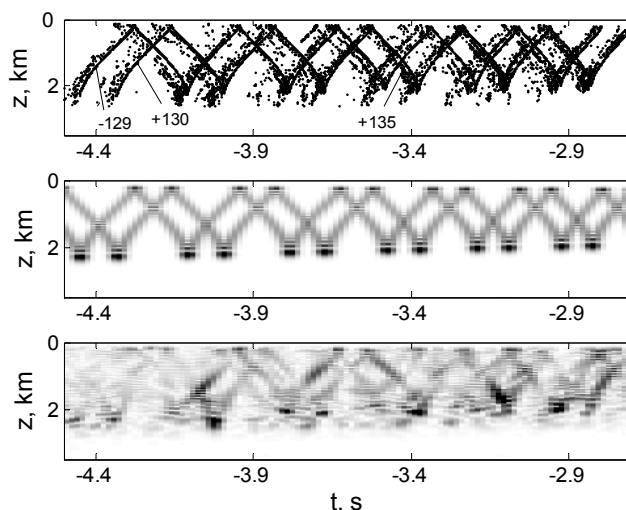


**Fig. 2.** The same as in Fig. 2 but for another part of the received signal that is formed by flatter rays.

In Ref. 3 it was shown that in the presence of large-scale inhomogeneities of the temperature field – for example, caused by synoptic eddies – biases of ray travel times occur in such a way that segments of the timefront shift in time but do not change their forms. In other words, the segment shifts as a single whole. Therefore when performing acoustic monitoring of climatic variations of the mean temperature it is enough to measure the biases of segments but not that of individual rays.

Our idea is to “tune in” the antenna for recording the shift of a whole segment corresponding to a selected identifier  $\pm M$ . Denote by  $\tau(z)$  the dependence of the travel time of an *unperturbed* ray with a selected identifier on its vertical coordinate (depth) at the observation range. A pulse signal recorded by an antenna element set at a depth  $z_n$  denote by  $v_n(t)$ . Let us shift all these signals according to formula

$$\bar{v}_n(t) = v_n(t - \tau(z_n)). \quad (1)$$

Consider a sum signal  $v(t) = \sum_n \bar{v}_n(t)$ . In the unperturbed waveguide an intensity  $|v(t)|^2$  has a maximum at  $t = 0$  because at that moment all  $\bar{v}_n(t)$  interfere constructively. Besides,  $|v(t)|^2$  has a few other maxima corresponding to neighboring segments of the timefront that are “parallel” to the selected one. The maxima will be observed at times  $t$  equal to shifts of these “parallel” segments relative the selected one.

Our main assumption is as follows. We expect that due to the relative closeness of perturbed and unperturbed ray travel times with the same identifiers [2], stable maximum at  $t = 0$  will be observed not only in the unperturbed waveguide but in the perturbed one as well. In order to check this conjecture we carried out calculations of a transient wave field excited by a point source for a few realizations of the random perturbation  $\delta c$ . Using the method of parabolic equation we computed the complex amplitude of the wave field  $u(\omega, r, z)$  at a set of carrier frequencies  $\omega$ . The output signal of antenna  $v(t)$  was synthesized by formula

$$v(t) = \int d\omega dz u(\omega, r, z) s(\omega) e^{-i\omega(t + \tau(z))}, \quad (2)$$

where  $s(\omega)$  is a spectrum of an initially emitted pulse. The function  $\tau(z)$  was computed using a ray code. The integration over  $z$  models summation over all elements of antenna. The latter covers the whole waveguide cross-section.

By “tuning” antenna to any segment (by selecting an appropriate  $\tau(z)$ ) we expect to get a maximum of  $|v(t)|^2$  at the same time  $t = 0$ . Therefore in order to enhance the effect we can add the dependences  $|v(t)|^2$  corresponding to a few neighboring segments. The upper panel in Fig. 3 shows an average intensity  $|v(t)|^2$  obtained by “tuning” the antenna to 14 сегментов with identifiers  $(-137) \div (-131); (+132) \div (+138)$ . Results of numerical simulations confirms the presence of a clearly seen maximum of  $|v(t)|^2$  at  $t = 0$ .

As it has been indicated above, the presence of maximum at  $t = 0$  means that arrivals of perturbed rays in time-depth plain group in the vicinity of the unperturbed timefront. Let us illustrate this fact in the following way. Consider a dense fan of rays escaping a point source. Let  $t_m$  and  $z_m$  be a travel time and depth of the  $m$ -th ray at the observation range. Introduce “shifted” travel times defined as

$$\bar{t}_m = t_m - \tau(z_m). \quad (3)$$

The lower panel of Fig. 3 presents the distribution of  $\bar{t}_m$  computed using a ray code for a fan of 50000 ray at 3000 km from the source. This distribution have been obtained by averaging over 14 histograms constructed for  $\bar{t}_m$ , defined by Eq. (3) with  $\tau(z)$  corresponding to the same 14 identifiers as that considered in the upper panel. It is clearly seen that the plot, similar to that presenting  $|v(t)|^2$ , has a well resolved maximum at  $t = 0$ .

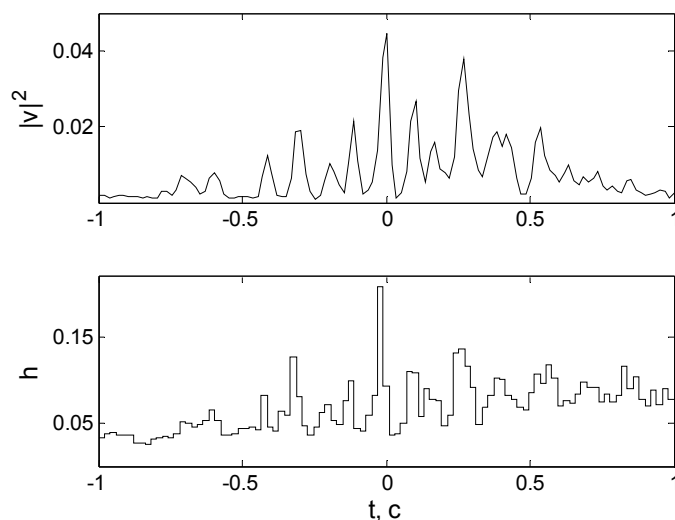


**Fig. 3.** *Upper panel:* averaged  $|v(t)|^2$ , obtained by “tuning in” the antenna to 14 segments of the timefront with identifiers  $(-137) \div (-131); (+132) \div (+138)$ . *Lower panel:* averaging over 14 histograms of shifted ray travel time distributions computed  $\tau(z)$  corresponding to the same 14 segments.

As it has been indicated above, climatic variations of temperature fields in the ocean cause shifts of the timefront segments. Therefore due to these variations the main maximum of  $|v(t)|^2$  corresponding to a single identifier or to a group of identifiers, will be shifted from  $t=0$ . The shifts can be used as input parameters when solving inverse problems. At multimegometer ranges the number of the timefront segments is large. Correspondingly, the difference in shifts of neighboring segments is relatively small. This justifies the summation of intensities  $|v(t)|^2$  corresponding to a few neighboring segments, as it has been done when constructing the plot presented in the upper panel of Fig. 3. However, for now it is not clear how to select the optimum number of segments for summation. This issue requires a further investigation.

The work was supported by the Grants No. 07-02-00255 and 05-05-64945 from the Russian Foundation for Basic Research, the Program "Coherent acoustic fields and signals" of Physical Sciences Division of Russian Academy of Sciences, and the Leading Scientific Schools grant 5200.2006.2.

#### REFERENCES

1. P. Worcester et al. A test of basin-scale acoustic thermometry using a large-aperture vertical array at 3250-km range in the eastern North Pacific Ocean // J. Acoust. Soc. Amer. 1999. V. 105(6). P. 3185–3201.
2. F. J. Beron-Vera et al. Ray dynamics in a long-range acoustic propagation experiment // J. Acoust. Soc. Amer. 2003. V. 114. P. 1226–1242.
3. A.L. Virovlyansky, A.Yu. Kazarova, L.Ya. Lyubavin. Reconstruction of the average ocean temperature from the measured travel times of sound pulses // Acoust. Phys. 2007. V. 53. No. 2. P. 181-189.